Activity of Northern Hemispheric storm tracks under global climate change

Yu.V. Martynova[1,2,4] **and V.N. Krupchatnikov**[1,3,4]

[1] Siberian Regional Hydrometeorological Research Institute, Novosibirsk, Russia
[2] Institute of Monitoring Climatic and Ecological Systems SB RAS, Tomsk, Russia
[3] Novosibirsk State University, Novosibirsk, Russia
[4] Institute of computational mathematics and mathematical geophysics SB RAS, Novosibirsk, Russia

E-mail: FoxyJ13@gmail.com

Abstract. This paper devoted to the study of the storm track behavior under increasing and further decreasing anthropogenic load. For our study we used global large scale climate system model of intermediate complexity. The climatic scenario RCP 8.5 was used as a scenario of anthropogenic load. We considered dynamics of the seasonal mean (winter — December, January, February; summer — June, July, August) v-variance at 250 mb ($(v'v')$ at 250 mb) as an indicator of the storm tracks activity and eddy momentum flux at 250 mb ($(u'v')$ at 250 mb) as an indicator of eddy kinetic energy behavior.

The study showed that areas of maximal storm track activity shift in the meridional direction to high latitude simultaneously with the atmospheric CO_2 concentration increase and shift back with further CO_2 concentration decrease. But the amplitude of the storm track activity doesn't change back to preindustrial value with the CO_2 concentration decrease. Thus the amplitude of the storm track activity exhibits weak hysteresis effect.

PACS numbers: 92.70.Cp, 92.70.Gt

Keywords: storm tracks, climate change, RCP 8.5

1. Introduction

Changes in the location, intensity or seasonality of major climatological features of the general circulation could be more important than average temperature changes, particularly where these changes might affect local hydrology, energy balances and etc.

The recent increase in global tropopause heights is closely associated with systematic temperature changes below and above the tropopause. Air temperature increases in the troposphere and decreases in the stratosphere. The pattern of warming and cooling also affects the zonal wind structure in the region of the subtropical upper troposphere and lower stratosphere (UTLS). At intermediate heights of the UTLS region (12-16 km) the tropics warming and the extratropics cooling lead to increase of meridional temperature gradient and zonal wind speed. Extratropical tropospheric eddies play a central role in this mechanism. The eddies tend to move eastward with the zonal flow and equator-ward toward the subtropics until they approach their critical latitudes, where their phase speed equals the speed of the background zonal flow.

The question is whether climate change will significantly affect the location and intensity of midlatitude storm tracks and associated jets. Because of the wave, mean-flow interaction in midlatitudes produces low-frequency variations in the latitude of the jets, it can be supposed that a modest climate change might significantly affect the position of jets and their associated storm tracks. The storm tracks are defined as the region of strong baroclinicity (maximum meridional temperature gradient), which are determined on the basis of eddy statistics like eddy fluxes of angular momentum, energy, and water (with the use of high band-pass filter). Extratropical eddies are the product of baroclinic instability, which shows itself particularly strongly during winter as a consequence of the strong pole-to-equator temperature gradient during it. In the Northern Hemisphere, there are two major storms in the region Atlantic and Pacific. The storm tracks:

- bring heavy rains and other hazardous weather phenomena in the middle latitudes;
- play an important role in the global energy cycle and the hydrological cycle.

Example: The winter climate of Europe and the Mediterranean is dominated by the weather systems of the midlatitude storm tracks. The behavior of the storm tracks is highly variable, particularly in the eastern North Atlantic, and has a profound impact on the climate of the Mediterranean region [5].

The study of the global warming effect on storm tracks and associated processes is an area of high interest for modern investigators. Both associated with storm tracks processes, such as frequency and rate cyclones and anticyclones, and more general common characteristics, such as v-variance, eddy momentum, heat and moisture fluxes are studied [1, 6, 10]. Currently, SRES are widely used to simulate a global climatic forcing. In studies devoted to storm tracks one climatic scenario (frequently SRES A1B) and one climatic model (e.g. [2]) or a climatic model ensemble (e.g. [13, 14]) are often used. Currently, most research is done only for conditions with increasing anthropogenic impact. We think that it is equally important to understand whether these changes to which climate system parameters were exposed due to the global climate change impact are reversible [11]. Some parameters, like precipitation, cloud cover, land permafrost area, demonstrate clear hysteresis behavior [4, 7].

In this paper we present results of our study of the storm track behavior under increasing and further decreasing anthropogenic load.

2. Experimental design

We performed our experiment using a global large scale climate system model of intermediate complexity "Planet Simulator" [8]. This model consists of several modules: atmosphere, ocean, land surface module, module of soil, sea ice and biosphere. In the experiment a horizontal resolution was T42, it is approximately 2.5 x 2.5 degrees. Vertical resolution for atmosphere was 10 equidistant σ-levels with the highest level at 10 mb, and for soil it was 5 depth levels at 0.4 m, 0.8 m, 1.6 m, 3.2 m, 6.4 m from surface. Time step was 20 minutes.

There is an ability to set any atmospheric CO_2 concentration in the "Planet Simulator". Using it we performed the experiment so that the atmospheric CO_2 concentration has changed for each next calculated year according to climatic scenario RCP 8.5. Climatic scenario we used reproduces both the atmospheric CO2 concentration increase due the anthropogenic pressure and its further decrease till return to preindustrial value (http://climate.uvic.ca/EMICAR5). Thus, the scenario of the atmospheric CO_2 concentration change consists of four parts:

(i) For a time period from 850 to 2005 CO_2 concentration was set according to the protocol "Historical simulations" of CMIP5.

(ii) During the 21–23 century CO_2 concentration was set according to the most aggressive scenario RCP 8.5.

(iii) During 24–29 century CO_2 was fixed on the level of the year 2300.

(iv) During 30–31 century CO_2 was returned to the preindustrial value. At this period during the first 100 years CO_2 concentration was decreasing linearly to preindustrial value and then fixed.

For the study of storm-track dynamics we selected following 9 time periods (Fig. 1). Zeroth period (1751–1760) is characterized by the equilibrium state of the climate system before the CO_2 increase. First period (1991–2000) was selected at the beginning of CO_2 concentration increase time period, second (2101–2110) was in the middle of this period, third (2191–2200) was at the end of this period. Fourth period (2691–2700) was selected for the conditions of equilibrium state of climate system with the extremely high CO_2 concentration. Fifth (3011–3020), sixth (3051–3060) and seventh (3111–3120) periods were selected for the atmospheric conditions at the beginning of CO_2 concentration decrease, in the middle of this period and at the end of this period, respectively. The last, eighth, period (3191–3200) was selected for the climate system conditions at the end of the simulation when CO_2 concentration has returned to the preindustrial state.

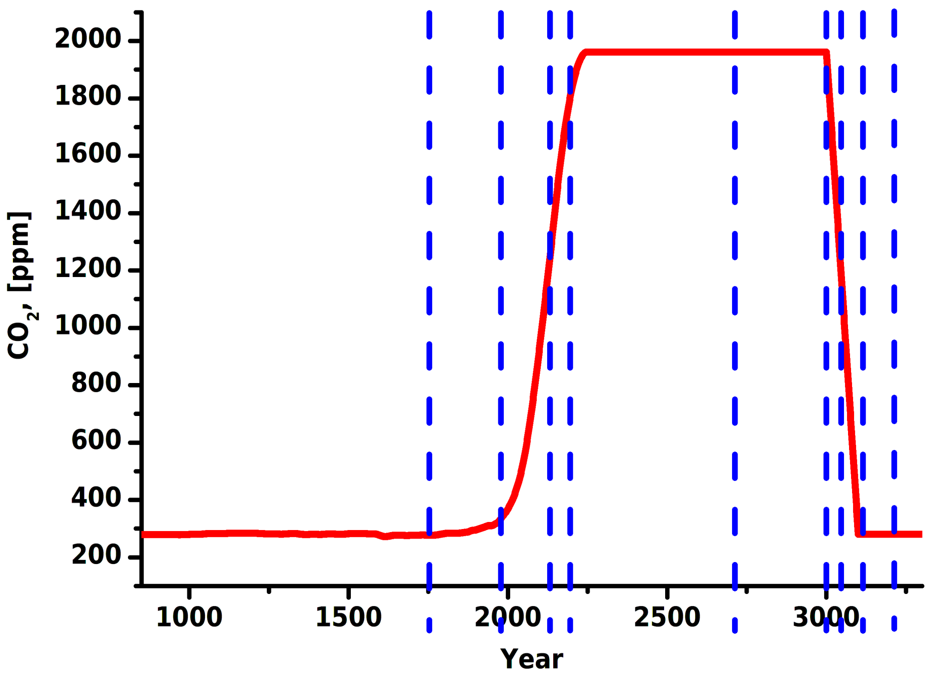

Figure 1. Reproduced both the atmospheric CO_2 concentration increase and following its decrease with the return it to preindustrial value climatic scenario (*http://climate.uvic.ca/EMICAR5*).

In this study we considered dynamics of the seasonal mean (winter – December, January, February; summer – June, July, August) v-variance at 250 mb (($v'v'$) at 250 mb) as an indicator of the storm tracks activity and eddy momentum flux at 250 mb (($u'v'$) at 250 mb) as an indicator of eddy kinetic energy behavior [6, 10]. To define these parameters we performed following sequence of calculations. First, u- and v-velocity data were filtered at each of the nine time periods to separate medium-scale waves (i.e. with periods 2–8 days) [3]. Then using filtered data for each season, mean ($v'v'$) and ($u'v'$) at 250 mb were calculated [6, 10].

3. Results

We focused on areas of maximal storm track activity. Because the atmospheric dynamics of winter and summer seasons varies, we considered these seasons separately. To examine the dynamics of the storm track activity in the zonal direction Hovmöller diagrams were constructed for the 10-years mean variance of meridional velocity ($v'v'$) at 250 mb, as an indicator of baroclinicity. Here we need to note that v-variance is a part of the eddy kinetic energy. The figure 2 shows these diagrams for winter and summer seasons. In these diagrams X axes presents the number of our time periods, Y axes is the latitude.

For both seasons the diagrams show a shift of areas of maximal storm track activity to high latitudes simultaneously with the CO_2 concentration increase. Furthermore, unlike the winter season the summer one demonstrates the reduce of the storm track activity besides the shift Hovmöller diagram. As for the energy, baroclinic weather layer (tropospher) is less active in summer than in winter. When atmospheric CO_2 concentration decreases and returns to preindustrial value, the areas of maximal storm track activity are shifted back to the preindustrial location for both seasons. The summer storm track activity tends to its preindustrial value but the winter storm track activity tends to less value then preindustrial. Here CO_2 concentration has returned to preindustrial value, but storm track activity has not and continues to decline.

(a) (b)

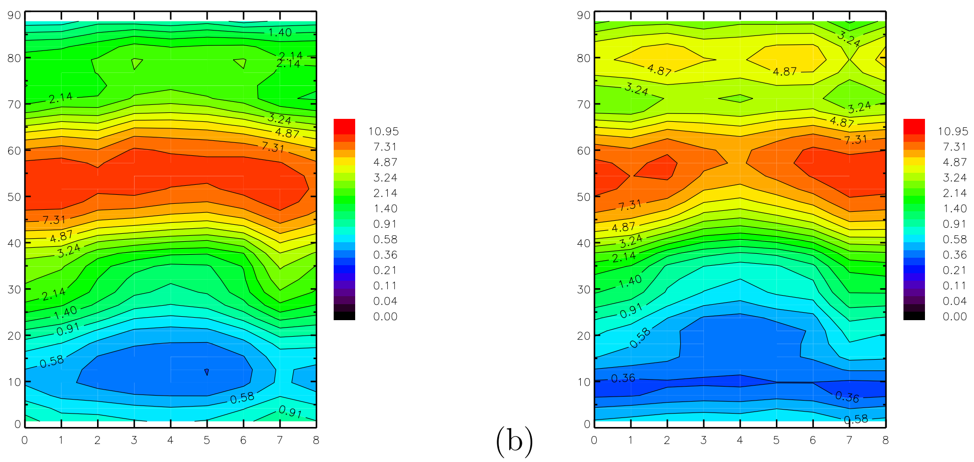

Figure 2. Hovmöller diagrams of meridional averaged 10-years mean variance of meridional velocity $(v'v')$ at 250 mb for the winter (a) and for the summer (b) seasons.

To study the change of a maximal storm track activity distribution in the meridional direction, we constructed another Hovmöller diagrams. Diagrams in figure 2 show that maximal storm track activity occurs over 54–55 N. In figure 3 Hovmöller diagrams of 10-years mean variance of meridional velocity $(v'v')$ at 54.4 N for winter and summer seasons are presented. X axes is the longitudes, Y axes is the number of the time periods. It is shown that the response of Atlantic storm track to CO_2 concentration change is stronger then the response of Pacific storm track. For a winter season Atlantic storm track amplitude raises with the CO_2 concentration increase, and it reduces with the CO_2 concentration decrease. Here the mentioned above phenomenon appears again. Atlantic storm track amplitude doesn't return to preindustrial value, and it continues to decline while the atmospheric CO_2 concentration obtains the preindustrial value and fixed on it. Pacific storm track amplitude reduces with the CO_2 concentration increase and raises with the CO_2 concentration decrease. Like the Atlantic storm track, Pacific storm track amplitude doesn't return to preindustrial value. For a summer season the amplitudes of both Atlantic and Pacific storm tracks reduce with the CO_2 concentration increase and raise with the CO_2 concentration decrease.

The reason of such climate system behavior is the fast return of atmospheric CO_2

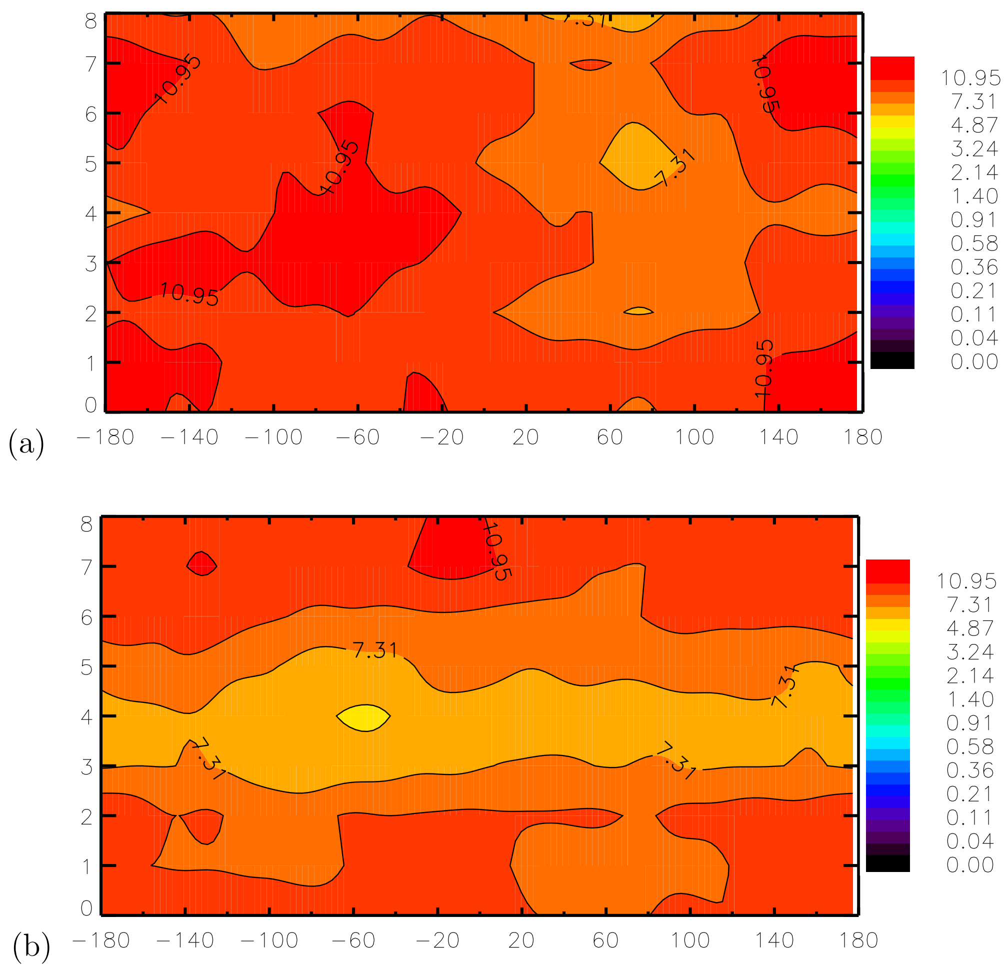

Figure 3. Hovmöller diagrams of 10-years mean variance of meridional velocity ($v'v'$) at 54.4 N and 250 mb for winter (a) and summer (b) seasons.

concentration, and as a consequence radiative forcing, to preindustrial value, leaving behind a slower, so-called recalcitrant, component [9]. The model "Planet Simulator" has a module of vegetation dynamics. It is a potential sources of hysteresis behavior of climate system. Here we considered the carbon cycle, which has own fast and slow components. The fast component can be readily driven by modifying of the atmospheric CO_2 concentration. Unlike the fast component slow, recalcitrant, one has a different spatial structure and cannot be return fully to preindustrial state by the same CO_2 concentration manipulation.

To highlight transport of momentum by eddies of synoptic time scale for both seasons we consider eddy momentum flux ($u'v'$) at 250 mb, (fig. 4). Hovmöller diagrams of eddies momentum flux demonstrate that the influence of the CO_2 concentration change to these fluxes for a winter season stronger then for a summer. It naturally follows from baroclinic activity increase. Absolute value of these fluxes raises with the CO_2 concentration increase and it reduces with the CO_2 concentration decrease.

There are two kinds of wave breaking: anti-cyclonic wave breaking (AWB) and

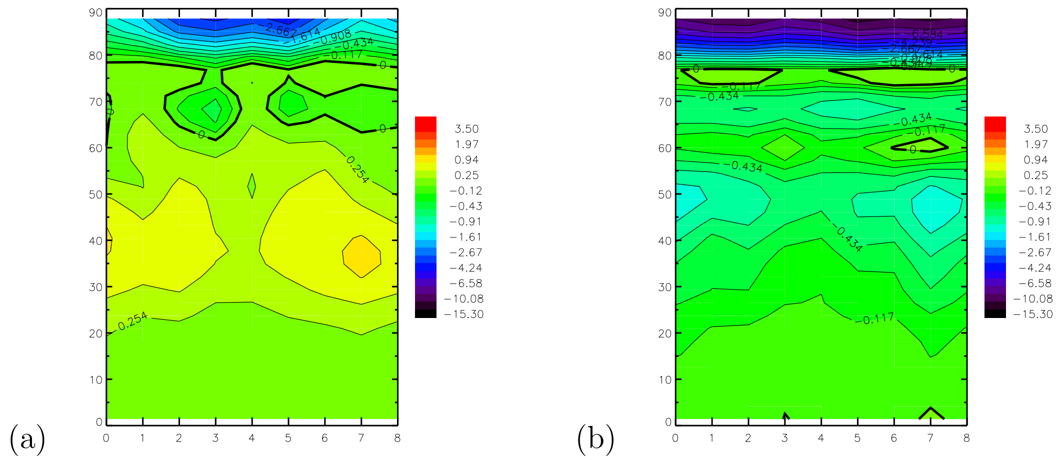

Figure 4. Hovmöller diagrams of meridional averaged 10-years mean poleward eddy momentum flux ($u'v'$) at 250 mb for the winter (a) and for the summer (b) seasons.

cyclonic wave breaking (CWB) [12]. The AWB is an equatorward wave breaking of the main westerly jet. CWB corresponds to a polewards wave breaking of it. In general AWB corresponds to an equatorward fluxes of wave activity (EliassenPalm fluxes). Similarly CWB corresponds to poleward flux of wave activity. Sign of the eddy momentum fluxes indicates a type of the wave breaking and depends on the spatial scales of the waves. Long (short) waves break anticyclonic type (cyclonic type) leading poleward (equatorward) shift of the jet. The transition from one type of breaking to another usually occurs at wave numbers 6–8 and depends on the background flow. It's known, that in first approximation the poleward momentum flux takes the opposite sign to meridional wavenumber. Thus associated with a equatorward propagating wave packet will be an poleward momentum flux, and vice versa. However, there is no well-established theory to explain it.

The effect on the zonal mean flow can be seen by writing the equation for the zonal mean momentum in term of EliassenPalm fluxes. A convergence of the wave activity leads to flow deceleration. AWB, which corresponds to an equatorward convergence of wave activity of the main westerly flow, thus gives rise to flow deceleration in that region, actually shifting the core of the eddy-driven jet to Pole. At the same time CWB leads to an equatorwards shift tendency of the jet.

4. Conclusion

Summing up the above we can conclude that in our case the variation of atmospheric CO_2 concentration significantly affects storm track behavior. In general the areas of maximal storm track activity shift in the meridional direction to high latitude simultaneously with the atmospheric CO_2 concentration increase and shift back with further CO_2 concentration decrease. But the amplitude of the storm track activity doesn't change back to preindustrial value with the CO_2 concentration decrease. At the end of simulations when CO_2 concentration is already returned to preindustrial value and fixed, the storm track amplitude continues to decline. Thus the amplitude of the storm track activity exhibits weak hysteresis effect. We associate this effect with a presence of so-called recalcitrant component in the climate system. This component is slow and cannot be driven by atmospheric CO_2 concentration variation only. The obtained storm track behavior is very interesting and requires further detailed study.

Acknowledgments

This work is partially supported by the Ministry of education and science of the Russian Federation (contract #8345), SB RAS project VIII.80.2.1, RFBR grants #11-05-01190a, 13-05-00480, and integrated project SB RAS #131.

References

[1] Akperov M G and Mokhov I I 2013 Estimates of the sensitivity of cyclonic activity in the troposphere of extratropical latitudes to changes in the temperature regime *Izvestiya, Atmospheric and Oceanic Physics* **49** 113–120

[2] Bengtsson L and Hodges K I 2006 Storm tracks and climate change *J. Climate* **19** 3518–3543

[3] Blackmon M L 1976 A climatological spectral study of the 500 mb geopotential height of the Northern Hemisphere *J. Atmos. Sci.* **33** 1607–1623

[4] Boucher O *et al* 2012 Reversibility in an Earth System model in response to CO_2 concentration changes *Environ. Res. Lett.* **7** 124013

[5] Brayshaw D J, Hoskins B and Blackburn M 2011 The Basic Ingredients of the North Atlantic Storm Track. Part II: Sea Surface Temperatures. *J. Atmos. Sci.* **68** 1784–1805

[6] Chang E K M, Yanjuan Guo, Xiaoming Xia and Minghua Zheng 2012 Storm-Track Activity in IPCC AR4/CMIP3 Model Simulations *J. Climate* **26** 246–260

[7] Eliseev A V, Demchenko P F, Arzhanov M M and Mokhov I I 2013 Transient hysteresis of near-surface permafrost response to external forcing *Clim. Dynamics* doi: 10.1007/s00382-013-1672-5

[8] Fraedrich K, Jansen H, Kirk E, Luksch U and Lunkeit F 2005 The Planet Simulator: Towards a user friendly model *Meteorol. Zeitschrift* **14** 299–304

[9] Held I *et al* 2009 Probing the fast and slow components of global warming by returning abrupty to preindustrial forcing *J. Climate* **23** 2418–2427

[10] Hoskins B J and Valdes P J 1990 On the existence of storm-tracks *J. Atmos. Sci.* **47** 1854–1864

[11] Matthews H D 2010 Can carbon cycle geoengineering be a useful complement to ambitious climate mitigation? *Carbon management* **1** 135–144

[12] Thorncroft C D, Hoskins B J and McIntyre M E 1993 Two paradigms of baroclinic-wave life-cycle behavior *Quart. J. Roy. Meteor. Soc.* **119** 17–55

[13] Ulbrich U *et al* 2008 Changing Northern Hemisphere Storm Tracks in an Ensemble of IPCC Climate Change Simulations *J. Climate* **21** 1669-1679

[14] Yin J H 2005 A consistent poleward shift of the storm tracks in simulations of 21st century climate *Geophys. Res. Lett.* **32** L18701